

Stress-Induced Densification of Glassy Polymers in the Subyield Region

ALEKSEY D. DROZDOV

Institute for Industrial Mathematics, 4 Hanachtom Street, Beersheba 84311, Israel

Received 15 June 1998; accepted 12 June 1999

ABSTRACT: Constitutive equations are derived for the viscoelastic response of amorphous glassy polymers in the region of subyield deformations. The model treats an amorphous polymer as a composite material consisting of an ensemble of flow units, immobile holes, and clusters of interstitial free volume moving through a network of long chains to and from voids. Changes in macropressure lead to an increase in the equilibrium concentration of interstitial free volume that, in turn, induces diffusion of free-volume elements from holes. The mass flow results in dissolution of voids that is observed as time-dependent densification of a glassy polymer. It is demonstrated that the model correctly predicts stress relaxation and a decrease in the specific volume observed in uniaxial tensile and compressive tests on polycarbonate at room temperature. © 1999 John Wiley & Sons, Inc. *J Appl Polym Sci* 74: 1705–1718, 1999

Key words: glassy polymers; mechanically induced densification; concept of traps; free-volume theory; composite materials

INTRODUCTION

This study is concerned with stress–strain relations for the viscoelastic behavior of amorphous glassy polymers that account for mechanically induced densification in the subyield region. The objective is to derive a constitutive model that can predict the following phenomena observed in uniaxial relaxation tests.¹ (1) Under tensile loads, the specific volume increases immediately after application of forces and slowly decreases afterward. (2) Under compressive loads, the specific volume decreases at the initial instant and proceeds to decrease with time, despite the stress relaxation.

Time-dependent response of amorphous polymers reflects rearrangement of segments in long chains. Below the glass transition temperature

Θ_g , this process requires cooperative dynamics of chain molecules, when scores of neighboring strands change their position simultaneously.² This picture is confirmed by measurements of dielectric relaxation and NMR spectroscopy in glass-forming liquids.^{3,4} A disordered medium is treated as an ensemble of cells (cooperatively rearranging regions or flow units³). Each region is a globule consisting of long and short chains and free-volume clusters.⁵ The characteristic size of a relaxing region in the vicinity of the Θ_g amounts to a few nanometers.⁶

Relaxation in an amorphous polymer at a temperature $\Theta > \Theta_g$ is thought of as a diffusion of rearranging regions on a free-energy hypersurface from one local potential well to another.⁷ According to the concept of ergodicity breaking,⁸ the ruggedness of the energy landscape increases with a decrease in temperature, and the phase space is decomposed into uncoupled cages at the Θ_g . Below Θ_g , a rearranging region cannot leave its cage, but can only hop to higher energy levels. The hops occur at random times, and the duration

Contract grant sponsor: Israeli Ministry of Science; contract grant numbers 9641-1-96 and 1202-1-98.

Journal of Applied Polymer Science, Vol. 74, 1705–1718 (1999)

© 1999 John Wiley & Sons, Inc.

CCC 0021-8995/99/071705-14

of a hop is assessed as a few picoseconds.⁴ Because the characteristic time of relaxation in the α region is about 1 s, flow units spend most time at the bottom levels of their traps near the points of minima for their free energies, which implies that the potential energy of a cage entirely determines the behavior of a trapped relaxing region.³

According to the transition-state theory,^{9–11} some liquidlike state exists on the energy landscape, where flow units change their configurations. Rearrangement occurs when a relaxing region reaches this reference state. The depth of a potential well where a flow unit is located with respect to the reference state is characterized by its energy w . For definiteness, we set $w = 0$ for the reference state and $w > 0$ for an arbitrary trap.

Two types of free-volume elements are distinguished¹²: (1) a hole (a micro-void frozen in the network), and (2) an interstitial free volume (clusters of free volume diffusing through a temporary network to and from holes).

In the Macedo–Litovitz theory,¹³ immobile holes model free-volume clusters the potential energies of which exceed those for thermal fluctuations, whereas interstitial free volumes represent elements of which barriers for redistribution are less than local fluctuations of energy caused by micro-Brownian motion.

Immobile voids are assumed to be randomly distributed in the bulk medium and filled with a gas (a mixture of air, monomer units, and molecules of plasticizer). By using observations of positron annihilation lifetime spectroscopy and fluorescent probe studies, the average hole radius R is estimated as several Å (0.35 nm for polycarbonate¹⁴ and 0.4 nm for polystyrene¹⁵). The gas pressure in a hole p is determined by the Laplace law

$$p = \frac{2Y}{R} \quad (1)$$

where Y is the surface tension. Accepting the value $Y = 0.034$ Pa m,¹⁶ we obtain $p = 170$ MPa for polystyrene, which substantially exceeds the yield stress. This implies that external loads practically do not affect dilatation of holes. This conclusion is confirmed fairly well by observations for polycarbonate in the subyield region.¹⁷

We assume that any rearranging region contains only one immobile spherical void, and the radii of all holes coincide. The latter hypothesis

contradicts some recent observations^{14,15,18} that reveal that volumes of voids are randomly distributed. It is chosen because (i) this assumption essentially simplifies the analysis, and (ii) there is no reliable way to measure the distribution of holes.¹⁹

Because the average size of a flow unit substantially exceeds that for a void (at least by an order), diffusion of free-volume clusters is analyzed in the vicinity of an individual hole (modeled as a spherical opening in an infinite space). This means that phenomena associated with macroscopic sizes of specimens are not taken into account. The latter is confirmed by experimental data²⁰ demonstrating that diffusion of free volume in and out of the boundaries of specimens cannot describe vitrification of polymers.

According to the Williams–Landel–Ferry (WLF) equation,²¹ the total free-volume fraction at the glass transition temperature Θ_g (when both types of free-volume clusters are accounted for) is about 2.5%. This implies that the volume fraction of interstitial free volume is relatively small, and a glassy polymer may be treated as a dilute solution of mobile free-volume clusters in a network of long chains. For isothermal loading, the equilibrium concentration of this solution χ_{eq} is determined by macropressure P only,

$$\chi_{\text{eq}}(P) = \chi_{\text{eq}}^0 + \Psi(P) \quad (2)$$

where χ_{eq}^0 is the equilibrium concentration of interstitial free volume in a stress-free medium, and the material function Ψ satisfies the condition

$$\Psi(P) > 0 \quad (P \neq 0), \quad \Psi(0) = 0 \quad (3)$$

Formula (3) means that any (positive or negative) volume deformation of a bulk medium activates a polymer and increases the equilibrium concentration of free volume. This contradicts simplified constitutive models based on the free-volume concept, which presumes that hydrostatic tension decreases relaxation times, whereas hydrostatic compression leads to their growth. In the framework of the free-volume theory,²² assumption (3) is confirmed fairly well by experimental data for poly(vinyl chloride), which demonstrate that (i) relaxation times decrease with the growth of longitudinal load both in tensile and compressive tests,²³ and (ii) retardation times for densified specimens exceed those for nondensified sam-

ples.²⁴ These observations may be explained by the Struik model,²⁵ according to which subyield strains in the vicinity of a hole (at tension, as well as at compression) lead to fracture of the van der Waals bonds and activate the microcavitation mechanism.

When external loads are applied to a specimen, pressure alters and engenders changes in the equilibrium concentration of interstitial free volume. The solution becomes subsaturated, which results in mass flux from voids to flow units. Diffusion of free-volume clusters from holes decreases their volume, which is revealed as mechanically induced densification of a glassy polymer.

In tensile relaxation tests on compressible specimens, an initial positive jump in the specific volume decreases with time because of stress relaxation and diffusion-driven dissolution of voids. In compressive tests, loads engender an initial negative jump in the specific volume. Because of stress relaxation, the stresses decrease, which results in some growth of the specific volume with time. On the other hand, diffusion of free-volume clusters from holes causes a decrease in their volume. When dissolution of voids driven by diffusive flow dominates volume recovery caused by stress relaxation, the specific volume of a polymer decreases with time. This scenario of densification is confirmed by experimental data for polycarbonate,¹ which demonstrate that the rate of decrease in the specific volume at tension essentially exceeds that at compression. The aim of this work is to provide a quantitative analysis of this phenomenon.

KINETICS OF COOPERATIVE REARRANGEMENT

Rearrangement of flow units is treated as a sequence of random hops driven by thermal fluctuations.¹¹ The probability for a flow unit to reach (in an arbitrary hop) the energy level that exceeds the bottom level of its trap by ω reads

$$\pi(\omega) = A \exp(-A\omega)$$

where A is a material constant.^{5,27,28} The exponential decay of the probability density for reaching high energy levels is justified by the extreme-value statistics.²⁹

Because rearranging regions spend most time at the bottom levels of their potential wells, the

probability of reaching the reference state in an arbitrary hop is given by

$$\Pi(w) = \int_w^\infty \pi(\omega) d\omega = \exp(-Aw)$$

The average rate of hops Γ is assumed to depend on the current temperature Θ only. Multiplying Γ by the probability of reaching the liquidlike state in a hop $\Pi(w)$, we arrive at the Eyring formula³⁰ for the rate of rearrangement for a flow unit trapped in a cage with potential energy w ,

$$L(w) = \Gamma \exp(-Aw) \quad (4)$$

Denoted by Ξ_0 the concentration of traps (per unit mass) and by $\Xi(t, \tau, w)$ the concentration at time t of traps with potential energy w which have rearranged before time $\tau \leq t$. The quantity $\Xi(t, \tau, w)$ is similar to the distribution function for active chains in the concept of temporary networks.³¹ This function entirely determines the rearrangement process. $\Xi(t, 0, w)$ is the number of traps with potential energy w filled at the initial instant $t = 0$ where flow units have not rearranged until time t ; $\Xi(t, t, w)$ is the number of traps with energy w at time t . The quantity

$$\frac{\partial \Xi}{\partial \tau}(t, \tau, w)|_{t=\tau} d\tau$$

is the number of flow units in traps with energy w rearranged within the interval $[\tau, \tau + d\tau]$, and the amount

$$\frac{\partial \Xi}{\partial \tau}(t, \tau, w) d\tau$$

is the number of these regions that have not reached the liquidlike state until time t . The number of initial flow units in traps with energy w reaching the reference state within the interval $[t, t + dt]$ reads

$$-\frac{\partial \Xi}{\partial t}(t, 0, w) dt$$

and the number of regions in traps with energy w that rearranged within the interval $[\tau, \tau + d\tau]$ and hop to the reference state within the interval $[t, t + dt]$ is given by

$$-\frac{\partial^2 \Xi}{\partial t \partial \tau}(t, \tau, w) dt d\tau$$

Equating the relative rates of reaching the reference state to the function $L(w)$, we arrive at the differential equations

$$\begin{aligned} \frac{\partial \Xi}{\partial t}(t, 0, w) &= -L(w)\Xi(t, 0, w) \\ \frac{\partial^2 \Xi}{\partial t \partial \tau}(t, \tau, w) &= -L(w) \frac{\partial \Xi}{\partial \tau}(t, \tau, w) \end{aligned}$$

The solutions of these equations read

$$\Xi(t, 0, w) = \Xi(0, 0, w) \exp[-L(w)t]$$

$$\frac{\partial \Xi}{\partial \tau}(t, \tau, w) = \frac{\partial \Xi}{\partial \tau}(t, \tau, w)|_{t=\tau} \exp[-L(w)(t - \tau)] \quad (5)$$

The function $\Xi(t, \tau, w)$ provides a detailed description of the distribution of traps with various potential energies. Conventional models^{5,28} employ a coarser measure, the probability density p of traps with potential energy w . Assuming the function p to be time-independent, we obtain

$$\Xi(t, t, w) = p(w)\Xi_0 \quad (6)$$

The number of flow units (per unit mass) in traps with potential energy w that reach the liquidlike state within the interval $[t, t + dt]$ reads

$$-\frac{\partial \Xi}{\partial t}(t, \tau, w)|_{\tau=t} dt = L(w)p(w)\Xi_0 dt$$

Because the duration of a hop is neglected, this equality determines also the number of flow units in cages with potential energy w that land within the interval $[t, t + dt]$

$$\frac{\partial \Xi}{\partial \tau}(t, \tau, w)|_{\tau=t} dt = L(w)p(w)\Xi_0 dt \quad (7)$$

Substitution of expressions (6) and (7) into eq. (5) results in

$$\begin{aligned} \Xi(t, 0, w) &= p(w)\Xi_0 \exp[-L(w)t] \\ \frac{\partial \Xi}{\partial \tau}(t, \tau, w) &= L(w)p(w)\Xi_0 \exp[-L(w)(t - \tau)] \quad (8) \end{aligned}$$

MECHANICAL ENERGY OF AN ENSEMBLE OF FLOW UNITS

A rearrangement event is modeled as a hop of a flow unit from the bottom level of its potential well to the liquidlike state, where the unit forgets its previous configuration (totally relaxes), followed by a landing to the previous trap.²⁸ The natural (stress-free) configuration of a relaxing region after landing coincides with the actual configuration of the ensemble of rearranging regions. This implies that the nominal strain tensor (the strain tensor for transition from its natural configuration to the actual configuration at the current instant t) reads

$$\hat{\mathcal{E}}^*(t, \tau) = \hat{\mathcal{E}}(t) - \hat{\mathcal{E}}(\tau)$$

where $\hat{\mathcal{E}}(t)$ is the strain tensor for transition from the initial configuration to the actual configuration of a rearranging region, and τ is the last instant before the current time t when the region was rearranged.

We treat a flow unit as an isotropic linear elastic medium with the mechanical energy

$$\begin{aligned} U_0(t, \tau) &= \frac{1}{2} \{K_0[\mathcal{E}^*(t, \tau)]^2 \\ &\quad + 2G_0 \hat{\mathcal{E}}_d^*(t, \tau) : \hat{\mathcal{E}}_d^*(t, \tau)\} \end{aligned}$$

where K_0 and G_0 are analogs of the bulk and shear moduli for a rearranging region, \mathcal{E}^* and $\hat{\mathcal{E}}_d^*$ are the first invariant and the deviatoric part of the strain tensor \mathcal{E}^* , and the colon denotes convolution.

The specific mechanical energy (per unit mass) of initial flow units that have not reached the reference state during the interval $[0, t]$ is calculated as

$$\begin{aligned} U(t, 0) &= \frac{1}{2} \int_0^t \Xi(t, 0, w) dw [K_0 \mathcal{E}^2(t) \\ &\quad + 2G_0 \hat{\mathcal{E}}_d(t) : \hat{\mathcal{E}}_d(t)] \end{aligned}$$

and the specific mechanical energy of flow units that landed from the reference state within the interval $[\tau, \tau + d\tau]$ and have not rearranged until the current time t is given by

$$\begin{aligned} dU(t, \tau) &= \frac{1}{2} \int_0^t \frac{\partial \Xi}{\partial \tau}(t, \tau, w) dw [K_0(\mathcal{E}(t) - \mathcal{E}(\tau))^2 \\ &\quad + 2G_0(\hat{\mathcal{E}}_d(t) - \hat{\mathcal{E}}_d(\tau)) : (\hat{\mathcal{E}}_d(t) - \hat{\mathcal{E}}_d(\tau))] d\tau \end{aligned}$$

Summing these expressions, we find the specific mechanical energy of an ensemble of relaxing regions

$$\begin{aligned}
 U_1(t) = \frac{1}{2} & \left\{ [K_0 \mathcal{E}^2(t) \right. \\
 & + 2G_0 \hat{\mathcal{E}}_d(t) : \hat{\mathcal{E}}_d(t)] \int_0^\infty \Xi(t, 0, w) dw \\
 & + \int_0^t [K_0(\mathcal{E}(t) - \mathcal{E}(\tau))^2 + 2G_0(\hat{\mathcal{E}}_d(t) \\
 & - \hat{\mathcal{E}}_d(\tau)) : (\hat{\mathcal{E}}_d(t) - \hat{\mathcal{E}}_d(\tau))] d\tau \\
 & \left. \times \int_0^\infty \frac{\partial \Xi}{\partial \tau}(t, \tau, w) dw \right\}
 \end{aligned}$$

With reference to ref. 32, we assume that the specific energy of interaction between rearranging regions depends on the first invariant $\mathcal{E}(t)$ of the strain tensor $\hat{\mathcal{E}}(t)$. In the framework of linear elasticity, this energy reads

$$U_2(t) = \frac{1}{2} K_* \mathcal{E}^2(t)$$

where K_* is an analog of the bulk modulus. Summing the potential energies of traps and the energy of their interaction, we arrive at the strain energy density (per unit mass) of a glassy polymer

$$\begin{aligned}
 U(t) = \frac{1}{2} & \left\{ \left[K_* + K_0 \int_0^\infty \Xi(t, 0, w) dw \right] \mathcal{E}^2(t) \right. \\
 & + 2G_0 \hat{\mathcal{E}}_d(t) : \hat{\mathcal{E}}_d(t) \int_0^\infty \Xi(t, 0, w) dw \\
 & + \int_0^t [K_0(\mathcal{E}(t) - \mathcal{E}(\tau))^2 + 2G_0(\hat{\mathcal{E}}_d(t) \\
 & - \hat{\mathcal{E}}_d(\tau)) : (\hat{\mathcal{E}}_d(t) - \hat{\mathcal{E}}_d(\tau))] d\tau \\
 & \left. \times \int_0^\infty \frac{\partial \Xi}{\partial \tau}(t, \tau, w) dw \right\} \quad (9)
 \end{aligned}$$

CONSTITUTIVE RELATIONS FOR AN AMORPHOUS POLYMER

Equation (9) expresses the specific mechanical energy of an amorphous polymer in terms of the

strain tensor for the ensemble of flow units $\hat{\mathcal{E}}(t)$, but not in terms of the strain tensor for the bulk medium $\hat{\epsilon}(t)$. According to conventional theories of mixtures,³³ the strain tensor $\hat{\epsilon}(t)$ for transition from the initial configuration of the bulk medium to its actual configuration equals the sum of the strain tensor for the solid skeleton $\hat{\mathcal{E}}(t)$ and the strain tensor for holes $\hat{\epsilon}(t)$:

$$\hat{\epsilon}(t) = \hat{\mathcal{E}}(t) + \hat{\epsilon}(t) \quad (10)$$

Because mass transfer across the boundaries of voids does not change their shapes, the deviatoric part of the strain tensor $\hat{\epsilon}(t)$ vanishes, and

$$\hat{\epsilon}(t) = \frac{1}{3} \epsilon(t) \hat{I} \quad (11)$$

where ϵ is the first invariant of $\hat{\epsilon}$, and \hat{I} is the unit tensor. Substitution of expressions (10) and (11) into eq. (9) results in

$$\begin{aligned}
 U(t) = \frac{1}{2} & \left\{ \left[K_* + K_0 \int_0^\infty \Xi(t, 0, w) dw \right] (\epsilon(t) \right. \\
 & - \epsilon(t))^2 + 2G_0 \hat{\epsilon}(t) : \hat{\epsilon}(t) \int_0^\infty \Xi(t, 0, w) dw \\
 & + \int_0^t [K_0((\epsilon(t) - \epsilon(\tau)) - (\epsilon(t) - \epsilon(\tau)))^2 \\
 & + 2G_0(\hat{\epsilon}(t) - \hat{\epsilon}(\tau)) : (\hat{\epsilon}(t) \\
 & - \hat{\epsilon}(\tau))] d\tau \int_0^\infty \frac{\partial \Xi}{\partial \tau}(t, \tau, w) dw \quad (12)
 \end{aligned}$$

where $\hat{\epsilon}(t)$ is the deviatoric part of the strain tensor $\hat{\epsilon}(t)$.

At small strains, the first invariant σ and the deviatoric part \hat{s} of the Cauchy stress tensor $\hat{\sigma}$ are determined by the formulas³¹

$$\sigma(t) = 3\rho_0 \frac{\partial U(t)}{\partial \epsilon(t)} \quad \hat{s}(t) = \rho_0 \frac{\partial U(t)}{\partial \hat{\epsilon}(t)}$$

where ρ_0 is the initial mass density. Substitution of expression (12) into these equalities results in the constitutive equations

$$\begin{aligned} \sigma(t) &= 3\rho_0 \left\{ \left[K_* + K_0 \int_0^\infty \Xi(t, t, w) dw \right] [\epsilon(t) - \varepsilon(t)] \right. \\ &\quad \left. - K_0 \int_0^t [\epsilon(\tau) - \varepsilon(\tau)] d\tau \int_0^\infty \frac{\partial \Xi}{\partial \tau}(t, \tau, w) dw \right\} \\ \hat{s}(t) &= 2\rho_0 G_0 \left\{ \hat{e}(t) \int_0^\infty \Xi(t, t, w) dw \right. \\ &\quad \left. - \int_0^t \hat{e}(\tau) d\tau \int_0^\infty \frac{\partial \Xi}{\partial \tau}(t, \tau, w) dw \right\} \end{aligned} \quad (13)$$

Combining eqs. (8) and (13), bearing in mind that

$$\int_0^\infty p(w) dw = 1 \quad (14)$$

and introducing the notation

$$K = \rho_0(K_* + K_0\Xi_0) \quad G = \rho_0 G_0 \Xi_0$$

$$\eta = \frac{K_0\Xi_0}{K_* + K_0\Xi_0} \quad (15)$$

we find that

$$\begin{aligned} \sigma(t) &= 3K \left\{ [\epsilon(t) - \varepsilon(t)] - \eta \int_0^t [\epsilon(\tau) - \varepsilon(\tau)] d\tau \int_0^\infty L(w)p(w) \exp[-L(w)(t - \tau)] dw \right\} \\ \hat{s}(t) &= 2G \left\{ \hat{e}(t) - \int_0^t \hat{e}(\tau) d\tau \int_0^\infty L(w)p(w) \times \exp[-L(w)(t - \tau)] dw \right\} \end{aligned} \quad (16)$$

For isothermal loading, the distribution of traps with various potential energies w is described by the Gaussian function

$$p(w) = \frac{1}{\sqrt{2\pi}\Sigma} \exp\left[-\frac{(w - W)^2}{2\Sigma^2}\right] \quad (17)$$

where W is the mean potential energy of a relaxing region and Σ is the standard deviation of energy for a flow unit. According to the physical meaning of the potential energy w , eq. (17) is acceptable, provided that the probability of traps with negative energies is small compared to unity,

$$\int_{-\infty}^0 p(w) dw \ll 1 \quad (18)$$

The random energy model (17) was employed in the analysis of physical aging in disordered media.^{3,11,34} Among other expressions suggested to fit experimental data, we mention the exponential function,^{5,11} and the stretched Gaussian function.^{10,35} Substituting expressions (4) and (17) into eqs. (16) and introducing the notation

$$z = Aw \quad W_* = AW \quad \Sigma_* = A\Sigma$$

we arrive at the constitutive equations for an amorphous glassy polymer

$$\begin{aligned} \sigma(t) &= 3K \left\{ [\epsilon(t) - \varepsilon(t)] - \frac{\eta\Gamma}{\sqrt{2\pi}\Sigma_*} \int_0^t [\epsilon(\tau) - \varepsilon(\tau)] d\tau \int_0^\infty \exp\left[-\left(\frac{(z - W_*)^2}{2\Sigma_*^2} + z + \Gamma(t - \tau)\exp(-z)\right)\right] dz \right\} \\ \hat{s}(t) &= 2G \left\{ \hat{e}(t) - \frac{\Gamma}{\sqrt{2\pi}\Sigma_*} \int_0^t \hat{e}(\tau) d\tau \int_0^\infty \exp\left[-\left(\frac{(z - W_*)^2}{2\Sigma_*^2} + z + \Gamma(t - \tau)\exp(-z)\right)\right] dz \right\} \end{aligned} \quad (19)$$

Given a function $\varepsilon(t)$, stress-strain relations (19) are determined by six material constants: K , G , η , Γ , W_* , and Σ_* . To reduce the number of adjustable parameters, we assume in sequel that

$$\eta = 1 \quad (20)$$

According to eq. (15), this equality means that the energy of interaction between flow units is neglected.

Because the volume fraction of immobile holes Λ is small, the strain $\varepsilon(t)$ is given by

$$\varepsilon(t) = \Lambda \frac{V(t) - V_0}{V_0} \tag{21}$$

where V_0 and $V(t)$ are average volumes of a void at the initial and current time, respectively.

DIFFUSION OF INTERSTITIAL FREE VOLUME

We treat holes as mutually independent and analyze diffusion of interstitial free volume in the vicinity of an isolated void in an infinite space. The hole is thought of as a spherical cavity with the radius $R = R(t)$. In spherical coordinates $\{r, \theta, \phi\}$, the concentration of interstitial free-volume $\chi(t, r)$ (mobile free volume per unit volume of the bulk medium) satisfies the boundary problem

$$\frac{\partial \chi}{\partial t} = \frac{D}{r^2} \frac{\partial}{\partial r} \left(r^2 \frac{\partial \chi}{\partial r} \right) \quad \chi(0, r) = \chi_{eq}^0$$

$$\chi(t, \infty) = \chi_{eq}^0 \quad \chi(t, R(t)) = \tilde{\chi}_{eq}(t) \tag{22}$$

where D is a constant diffusivity and $\tilde{\chi}_{eq}(t) = \chi_{eq}(P(t))$. Mass flux through the boundary of a hole obeys the Fick law

$$\frac{dM}{dt}(t) = 4\pi DR^2(t)m_0 \frac{\partial \chi}{\partial r}(t, R(t))$$

where m_0 is the average mass of a mobile free-volume cluster, $M(t) = \frac{4}{3}\pi\rho(t)R^3(t)$ is the average mass of the cavity, and ρ is the current mass density of gas in the void. Assuming gas to be perfect and its motion to be adiabatic, we find that

$$\frac{p}{p^0} = \left(\frac{\rho}{\rho^0} \right)^\kappa$$

where p^0 and ρ^0 are the pressure and the mass density of gas before loading, and κ is Poisson's ratio (the ratio of the specific heat at a fixed pressure to that at a fixed volume). It follows from these equations that

$$\frac{\partial \chi}{\partial r}(t, R(t)) = \frac{(3\kappa - 1)\rho^0}{3\kappa D m_0} \left[\frac{R^0}{R(t)} \right]^{1/\kappa} \frac{dR}{dt}(t) \tag{23}$$

where R^0 is the average radius of a hole before loading.

The nonlinear initial boundary problem (22) and (23) is solved by using an approximate method developed in ref. 26. Omitting technical details, we arrive at the nonlinear integral equation for function $R(t)$

$$R(t) = R^0 \left\{ 1 - \frac{3m_0}{\rho^0(R^0)^3} \sqrt{\frac{D}{\pi}} \int_0^t \Psi(P(s))R^4(s) \times \left[\int_s^t R^4(\tau) d\tau \right]^{-1/2} ds \right\}^{\kappa/(3\kappa-1)} \tag{24}$$

It follows from eq. (24) that the function

$$T(t) = \int_0^t \left[\frac{R(s)}{R^0} \right]^4 ds \tag{25}$$

satisfies the integro-differential equation

$$\frac{dT}{dt}(t) = \left\{ 1 - \frac{6m_0R^0}{\rho^0} \sqrt{\frac{D}{\pi}} \left[\Psi(P(0))\sqrt{T(t)} + \int_0^t \frac{d\Psi}{dP}(P(s)) \frac{dP}{ds}(s) \sqrt{T(t) - T(s)} ds \right] \right\}^{4\kappa/(3\kappa-1)} \tag{26}$$

with the initial condition

$$T(0) = 0 \tag{27}$$

Setting

$$\Psi(P) = B|P|$$

where B is an adjustable parameter, and bearing in mind that $P = -\frac{1}{3}\sigma$, we present eq. (26) as

$$\frac{dT}{dt}(t) = \left\{ 1 - L \left[|\sigma(0)|\sqrt{T(t)} + \int_0^t \text{sign } \sigma(s) \frac{d\sigma}{ds}(s) \sqrt{T(t) - T(s)} ds \right] \right\}^{4\kappa/(3\kappa-1)} \tag{28}$$

where

$$L = \frac{2Bm_0R^0}{\rho^0} \sqrt{\frac{D}{\pi}}$$

It follows from eqs. (21), (25), and (28) that

$$\begin{aligned} \varepsilon(t) = \Lambda \left\langle \left\{ 1 - L \left[|\sigma(0)| \sqrt{T(t)} + \int_0^t \text{sign } \sigma(s) \right. \right. \right. \\ \left. \left. \left. \times \frac{d\sigma}{ds}(s) \sqrt{T(t) - T(s)} ds \right] \right\}^{3\kappa/(3\kappa-1)} - 1 \right\rangle \quad (29) \end{aligned}$$

The heat capacities for the hole free volume are assumed to coincide with those for air, which results in $\kappa = 1.4$. In this case, eqs. (28) and (29) are determined by two adjustable parameters, L and Λ , which are found by fitting observations in uniaxial tests.

UNIAXIAL EXTENSION OF A BAR

We introduce Cartesian coordinates with unit vectors \bar{e}_i and present the strain tensor $\hat{\varepsilon}$ in the form

$$\hat{\varepsilon}(t) = \epsilon_1(t)[\bar{e}_1\bar{e}_1 - \nu(t)(\bar{e}_2\bar{e}_2 + \bar{e}_3\bar{e}_3)]$$

where ϵ_1 is the longitudinal strain, ϵ_2 is the lateral strain, and $\nu = -\epsilon_2/\epsilon_1$ is Poisson's ratio. By substituting this expression into eqs. (19) and using the boundary condition in stresses on the lateral surface of the specimen, we find the longitudinal stress

$$\begin{aligned} \sigma_1(t) = 2G \left\{ [1 + \nu(t)]\epsilon_1(t) - \frac{\Gamma}{\sqrt{2\pi\Sigma_*}} \int_0^t \right. \\ \left. \times [1 + \nu(\tau)]\epsilon_1(\tau) d\tau \int_0^\infty \exp \left[- \left(\frac{(z - W_*)^2}{2\Sigma_*^2} \right. \right. \right. \right. \\ \left. \left. \left. + z + \Gamma(t - \tau)\exp(-z) \right) \right] dz \right\} \quad (30) \end{aligned}$$

Because σ_1 is the only nonzero component of the stress tensor, the first invariant of the stress tensor coincides with the longitudinal stress,

$$\sigma(t) = \sigma_1(t) \quad (31)$$

For an isothermal relaxation test with

$$\epsilon_1(t) = \begin{cases} 0, & t < 0 \\ \epsilon_1, & t \geq 0 \end{cases}$$

eq. (30) reads

$$\begin{aligned} E(t) = 2G \left\{ [1 + \nu(t)] - \frac{\Gamma}{\sqrt{2\pi\Sigma_*}} \int_0^t [1 + \nu(\tau)] d\tau \right. \\ \left. \times \int_0^\infty \exp \left[- \left(\frac{(z - W_*)^2}{2\Sigma_*^2} + z \right. \right. \right. \right. \\ \left. \left. \left. + \Gamma(t - \tau)\exp(-z) \right) \right] dz \right\} \quad (32) \end{aligned}$$

where

$$E(t) = \frac{\sigma_1(t)}{\epsilon_1} \quad (33)$$

is the current Young modulus.

It follows from eqs. (19) and (31) that the function $F(t) = \epsilon(t) - \varepsilon(t)$ obeys the integral equation

$$\begin{aligned} E(t)\epsilon_1 = 3K \left\langle F(t) - \frac{\Gamma}{\sqrt{2\pi\Sigma_*}} \int_0^t F(\tau) d\tau \right. \\ \left. \times \int_0^\infty \exp \left\{ - \left[\frac{(z - W_*)^2}{2\Sigma_*^2} + z \right. \right. \right. \right. \\ \left. \left. \left. + \Gamma(t - \tau)\exp(-z) \right] \right\} dz \right\rangle \quad (34) \end{aligned}$$

Comparison of eqs. (32) and (34) implies that

$$F(t) = \frac{2G}{3K} [1 + \nu(t)]\epsilon_1$$

which results in the formula

$$\varepsilon(t) = \left\{ [1 - 2\nu(t)] - \frac{2G}{3K} [1 + \nu(t)] \right\} \epsilon_1 \quad (35)$$

The elastic moduli G and K are expressed in terms of some average Young's modulus E_{av} and Poisson's ratio ν_{av} by the standard formulas

$$G = \frac{E_{av}}{2(1 + \nu_{av})} \quad K = \frac{E_{av}}{3(1 - 2\nu_{av})}$$

Combining these equalities with eq. (35), we obtain

$$\varepsilon(t) = 3\varepsilon_1 \frac{\nu_{av} - \nu(t)}{1 + \nu_{av}}$$

It follows from this equality and the initial condition $\varepsilon(0) = 0$ that

$$\nu_{av} = \nu(0) \tag{36}$$

and

$$\varepsilon(t) = 3\varepsilon_1 \frac{\nu(0) - \nu(t)}{1 + \nu(0)} \tag{37}$$

Formulas (28), (31), and (33) result in the integro-differential equation

$$\frac{dT}{dt}(t) = \left\{ 1 - L_0 \left[\sqrt{T(t)} + \int_0^t \text{sign } \sigma_1(s) \frac{dE_*}{ds}(s) \sqrt{T(t) - T(s)} ds \right]^{4\kappa/(3\kappa-1)} \right\} \tag{38}$$

where $L_0 = LE(0)|\varepsilon_1|$ and

$$E_*(t) = \frac{E(t)}{E(0)}$$

is the dimensionless Young modulus. According to eq. (29),

$$\log(-\varepsilon(t)) = \log \Lambda + \log \left\{ 1 - \left[1 - L_0 \left[\sqrt{T(t)} + \int_0^t \text{sign } \sigma(s) \frac{dE_*}{ds}(s) \sqrt{T(t) - T(s)} ds \right]^{3\kappa/(3\kappa-1)} \right] \right\} \tag{39}$$

where $\log = \log_{10}$.

COMPARISON WITH EXPERIMENTAL DATA

Adjustable parameters in governing equations are found by matching observations in uniaxial tensile and compressive relaxation tests for polycarbonate (PC GE) at room temperature. For a detailed description of the experimental procedure, see ref. 1. Because stress-strain relations (19) are linear, whereas glassy polymers reveal a nonlinear response in the subyield region, it is natural to assume that some material parameters become functions of the longitudinal strain ε_1 .

To determine the parameters G , W_* , and Σ_* , the following approximate technique is employed. First, Poisson's ratio $\nu(t)$ is found from measurements of the volume strain $\varepsilon(t)$ using the standard equation

$$\varepsilon = (1 - 2\nu)\varepsilon_1$$

The function $\nu(t)$ is approximated by the truncated Prony series

$$\nu(t) = \sum_{n=1}^N \nu_n \exp(-\lambda_n t) \tag{40}$$

Given $N = 4$ and λ_n ($\lambda_1 = 0$, $\lambda_2 = 10^{-2}$, $\lambda_3 = 10^{-3}$, $\lambda_4 = 10^{-4}$), the coefficients ν_n are determined by the least-squares method. Afterwards, the volume strain for voids ε is calculated by eq. (37). The function $\varepsilon(t)$ is depicted in Figures 1 and 2 together with its fitting by eqs. (37) and (40). These figures demonstrate that (i) eq. (40) with $N = 4$ ensures an acceptable matching of observations, and (ii) Poisson's ratio $\nu(t)$ weakly changes with time t [its relative increment $\Delta\nu(t) = (\nu(t) - \nu(0))/\nu(0)$ does not exceed 12%]. This implies that the function $\nu(t)$ in eq. (32) may be replaced by its average value ν_{av} . According to eqs. (36) and (40), the parameter ν_{av} reads

$$\nu_{av} = \sum_{n=1}^N \nu_n$$

The average Poisson ratio ν_{av} is plotted versus the longitudinal strain ε_1 in Figure 3. This figure

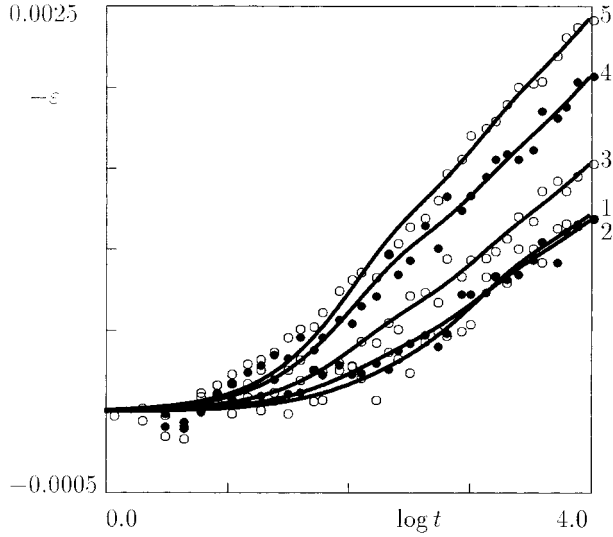


Figure 1 The volume strain of holes ε versus time t s for uniaxial extension of polycarbonate. Circles: experimental data.¹ Solid lines: their approximation by the model. Curve 1: $\varepsilon_1 = 0.01$; curve 2: $\varepsilon_1 = 0.015$; curve 3: $\varepsilon_1 = 0.02$; curve 4: $\varepsilon_1 = 0.025$; curve 5: $\varepsilon_1 = 0.03$.

shows that the dependence $\nu_{av}(\varepsilon_1)$ can be approximated by the linear function

$$\nu_{av}(\varepsilon_1) = a_0 + a_1|\varepsilon_1| \quad (41)$$

Replacing the function $\nu(t)$ in eq. (32) by its average value, we obtain

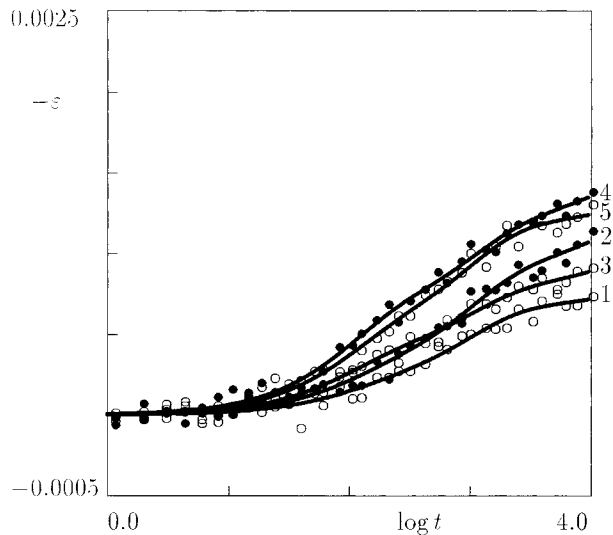


Figure 2 The volume strain of holes ε versus time t s for uniaxial compression of polycarbonate. Circles: experimental data.¹ Solid lines: their approximation by the model. Curve 1: $\varepsilon_1 = 0.01$; curve 2: $\varepsilon_1 = 0.015$; curve 3: $\varepsilon_1 = 0.02$; curve 4: $\varepsilon_1 = 0.025$; curve 5: $\varepsilon_1 = 0.03$.

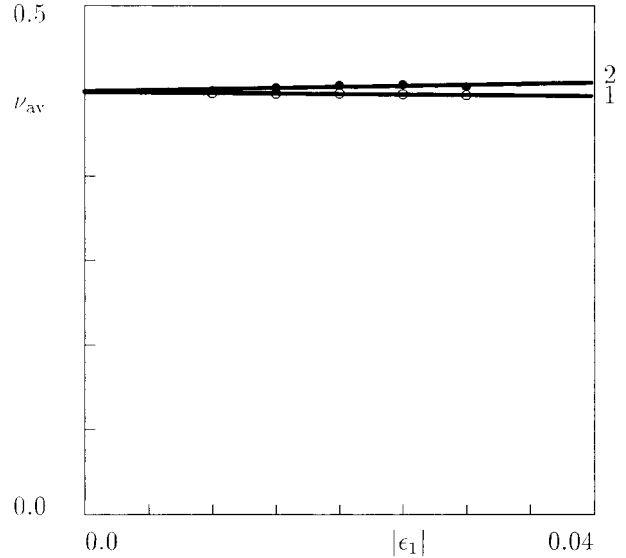


Figure 3 The average Poisson ratio ν_{av} versus the longitudinal strain ε_1 for polycarbonate. Circles: treatment of observations.¹ Solid lines: approximation of experimental data by eq. (41). Curve 1: extension, $a_0 = 0.4159$ and $a_1 = -0.0980$; curve 2: compression, $a_0 = 0.4169$ and $a_1 = 0.2060$.

$$E(t) = \frac{E_{av}}{\sqrt{2\pi}\Sigma_*} \int_0^\infty \exp\left\{-\left[\frac{(z - W_*)^2}{2\Sigma_*^2} + \Gamma t \exp(-z)\right]\right\} dz \quad (42)$$

where $E_{av} = 2G(1 + \nu_{av})$. To determine the parameters E_{av} , Γ , W_* , and Σ_* , we fit experimental data in relaxation tests with various longitudinal strains ε_1 by eq. (42). Given Γ , W_* , and Σ_* , the quantity E_{av} is found by the least-squares technique. Afterwards, the values of Γ , W_* , and Σ_* that minimize the discrepancies between observations and predictions of eq. (42) are calculated by using the method of steepest descent. Numerical analysis demonstrates that the parameters Γ and Σ_* are practically independent of the longitudinal strain ε_1 , whereas the average Young modulus E_{av} and the dimensionless mean energy W_* linearly decrease with $|\varepsilon_1|$,

$$E_{av}(\varepsilon) = E_{av}(0) - E'_{av}(0)|\varepsilon_1|$$

$$W_*(\varepsilon) = W_*(0) - W'_*(0)|\varepsilon_1| \quad (43)$$

Figures 4 and 5 show that the rate of drop in W_* for tension exceeds that for compression twice,

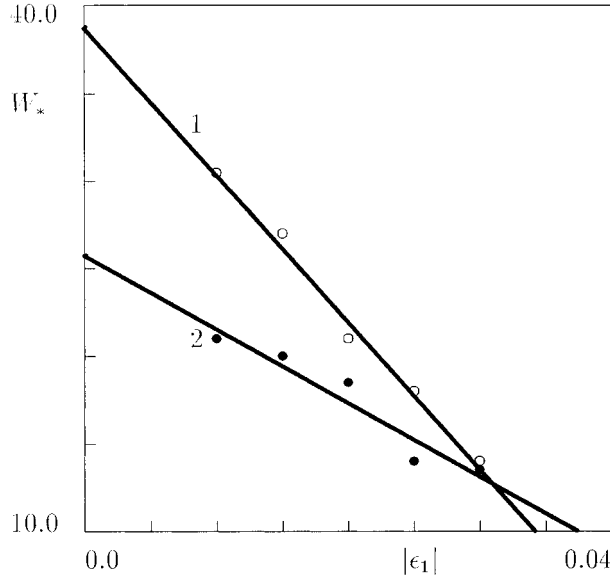


Figure 4 The dimensionless mean energy W_* versus the longitudinal strain ϵ_1 for polycarbonate. Circles: treatment of observations.¹ Solid lines: approximation of experimental data by eq. (43). Curve 1: extension, $W_*(0) = 38.9$ and $W'_*(0) = 840.0$; curve 2: compression, $W_*(0) = 25.8$ and $W'_*(0) = 420.0$.

whereas the rates of decline in E_{av} for tension and compression are close to one another.

To verify the model, we substitute expression (40) into eq. (32) and integrate the resulting

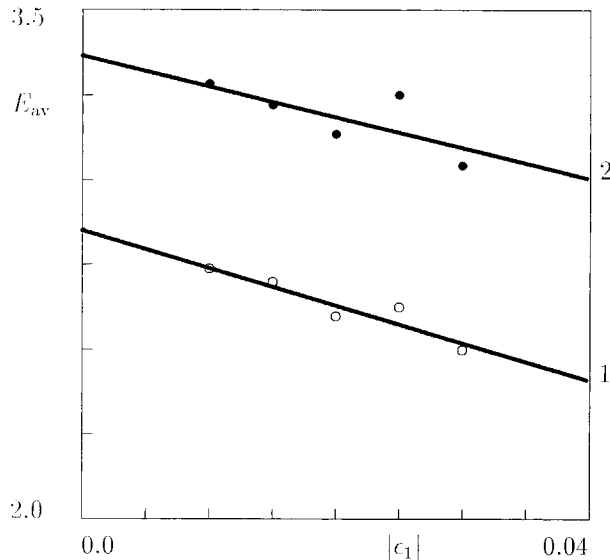


Figure 5 The average Young modulus E_{av} versus the longitudinal strain ϵ_1 for polycarbonate. Circles: treatment of observations.¹ Solid lines: approximation of experimental data by eq. (43). Curve 1: extension, $E_{av}(0) = 2.8525$ and $E'_{av}(0) = 11.072$; curve 2: compression, $E_{av}(0) = 3.3680$ and $E'_{av}(0) = 9.0680$.

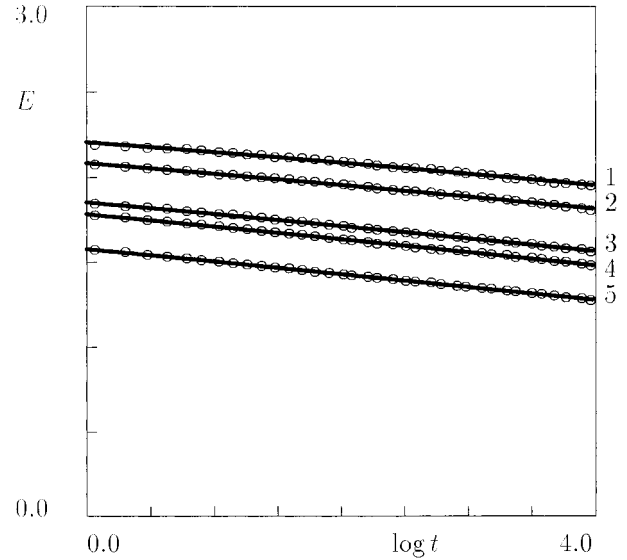


Figure 6 The Young modulus E GPa versus time t s for polycarbonate in tensile relaxation tests. Circles: experimental data.¹ Solid lines: predictions of the model with $\Gamma = 25.0 \text{ s}^{-1}$ and $\Sigma_* = 30.0$. Curve 1: $\epsilon_1 = 0.01$; curve 2: $\epsilon_1 = 0.015$; curve 3: $\epsilon_1 = 0.02$; curve 4: $\epsilon_1 = 0.025$; curve 5: $\epsilon_1 = 0.03$.

equality. Experimental data in tensile and compressive tests are plotted together with their approximations by the model in Figures 6 and 7. These figures demonstrate fair agreement between observations and results of numerical simulation.

Integro-differential eq. (38) with initial condition (27) is solved numerically, and the function $\varepsilon(t)$ is determined from eq. (39). The adjustable parameters L_0 and Λ are found from the condition of the best fit of the curves $\varepsilon = \varepsilon(t)$. The parameter L_0 is chosen to ensure that the slope of the graph $\log \varepsilon(\log t)$ coincides with that found from observations. Then the graph $\log \varepsilon(\log t)$ is shifted along the ordinate axis as a rigid body, and the parameter Λ is determined, which provides the best approximation of the experimental curve. Observations are plotted together with results of numerical simulation in Figures 8 and 9, which demonstrate an acceptable agreement between experimental data and their prediction.

The parameters L_0 and Λ are depicted versus the longitudinal strain ϵ_1 in Figures 10 and 11. The figures demonstrate that these quantities are approximated fairly well by the linear functions of $|\epsilon_1|$,

$$L_0(\epsilon_1) = b|\epsilon_1| \quad \log \Lambda(\epsilon_1) = c_0 + c_1|\epsilon_1| \quad (44)$$

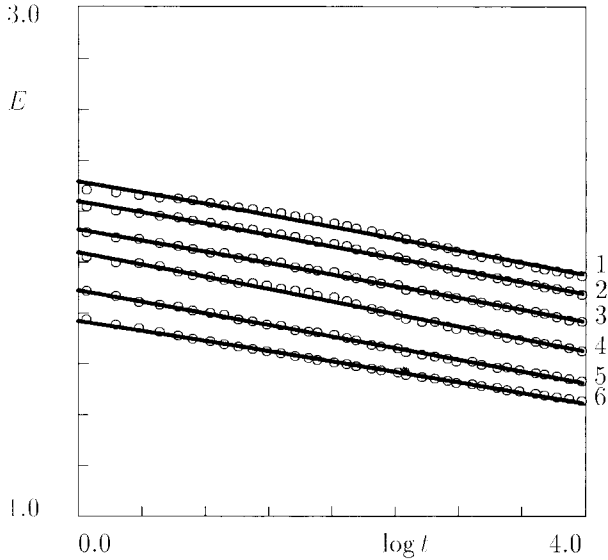


Figure 7 The Young modulus E GPa versus time t s for polycarbonate in compressive relaxation tests. Circles: experimental data.¹ Solid lines: predictions of the model with $\Gamma = 25.0 \text{ s}^{-1}$ and $\Sigma_* = 30.0$. Curve 1: $\epsilon_1 = 0.01$; curve 2: $\epsilon_1 = 0.015$; curve 3: $\epsilon_1 = 0.02$; curve 4: $\epsilon_1 = 0.025$; curve 5: $\epsilon_1 = 0.03$; curve 6: $\epsilon_1 = 0.035$.

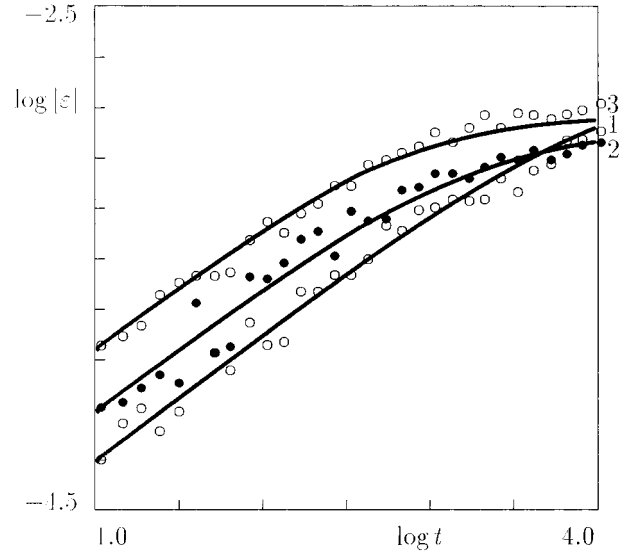


Figure 9 The volume strain of holes ϵ versus time t s for polycarbonate in compressive relaxation tests. Circles: experimental data.¹ Solid lines: their approximation by the model. Curve 1: $\epsilon_1 = 0.01$; curve 2: $\epsilon_1 = 0.02$; curve 3: $\epsilon_1 = 0.03$.

It follows from the first equality in eqs. (44) that the parameter L is independent of the longitudinal strain. Bearing in mind the connection between L and the self-diffusivity D , we arrive at

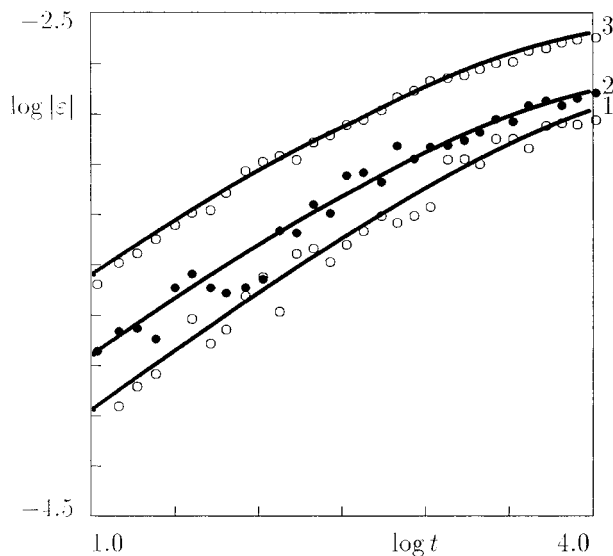


Figure 8 The volume strain of holes ϵ versus time t s for polycarbonate in tensile relaxation tests. Circles: experimental data.¹ Solid lines: their approximation by the model. Curve 1: $\epsilon_1 = 0.01$; curve 2: $\epsilon_1 = 0.02$; curve 3: $\epsilon_1 = 0.03$.

the conclusion that the coefficient D is independent of mechanical factors in the subyield region. This assertion is confirmed fairly well by matching observations in relaxation tests. Indeed, ac-

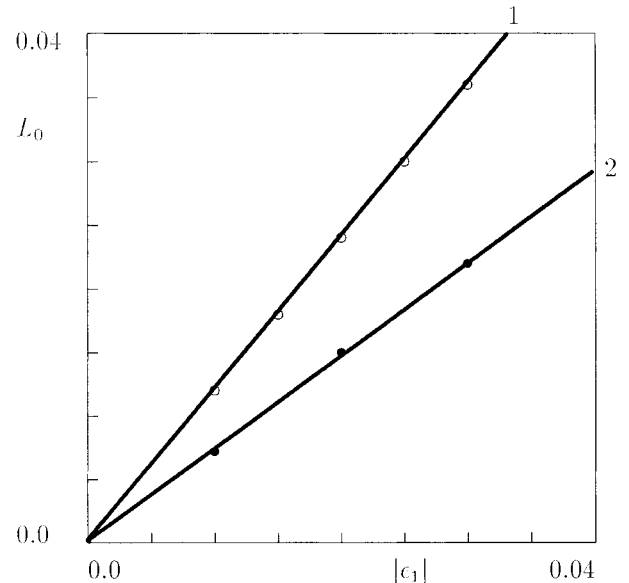


Figure 10 The parameter L_0 versus the longitudinal strain ϵ_1 for polycarbonate. Circles: treatment of observations.¹ Solid lines: approximation of experimental data by eq. (44). Curve 1: extension, $b = 1.200$; curve 2: compression, $b = 0.729$.

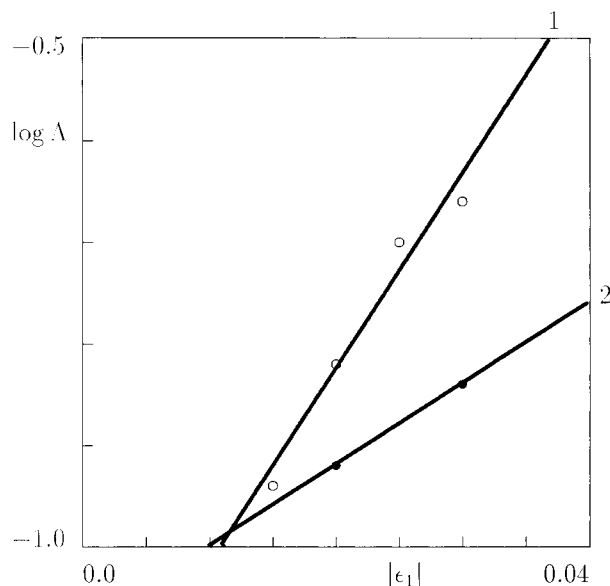


Figure 11 The parameter Λ versus the longitudinal strain ϵ_1 for polycarbonate. Circles: treatment of observations.¹ Solid lines: approximation of experimental data by eq. (44). Curve 1: extension, $c_0 = -1.212$ and $c_1 = 19.2$; curve 2: compression, $c_0 = -1.080$ and $c_1 = 8.0$.

cepting a conventional formula to express the parameter D in terms of the material viscosity ξ , we find that ξ is independent of strains. On the other hand, ξ is proportional to the relaxation time T , whereas the constancy of T at various longitudinal strains is demonstrated by the data depicted in Figures 6 and 7.

The second equality in eqs. (44) and Figure 11 reveal that the volume fraction of immobile voids (free-volume clusters) in a stress-free medium $\Lambda(0)$ is about 6–8%. These values coincide with measurements of the free-volume fraction in poly(vinyl acetate)³⁶ and poly(chlorotrifluoroethylene)³⁷ obtained by positron-annihilation lifetime spectroscopy.

CONCLUSIONS

Constitutive equations were derived for mechanically induced densification in amorphous glassy polymers at isothermal loading. The model combines the theory of traps for disordered media with the diffusion concept for free-volume clusters in a network of chain molecules. An amorphous polymer is treated as a composite material consisting of an ensemble of relaxing regions, inter-

stitial free volume, and immobile voids. Stress-strain relations (19) are developed for the viscoelastic response of glassy polymers at small strains and nonlinear integro-differential eqs. (28) and (29) are derived for dilatation caused by diffusion of free volume to and from holes. Adjustable parameters of the model are found by fitting experimental data for polycarbonate. It is demonstrated that constitutive equations correctly describe the viscoelastic behavior of an amorphous polymer and changes in its specific volume.

REFERENCES

- Colucci, D. M.; O'Connell, P. A.; McKenna, G. B. *Polym Eng Sci* 1997, 37, 1469.
- Adam, G.; Gibbs, J. H. *J Chem Phys* 1965, 43, 139.
- Dyre, J. C. *Phys Rev Lett* 1987, 58, 792.
- Dyre, J. C. *Phys Rev E* 1999, 59, 2458.
- Sollich, P. *Phys Rev E* 1998, 58, 738.
- Rizos, A. K.; Ngai, K. L. *Phys Rev E* 1999, 59, 612.
- Bässler, H. *Phys Rev Lett* 1987, 58, 767.
- Palmers, R. G. *Adv Phys* 1982, 31, 669.
- Goldstein, M. *J Chem Phys* 1969, 51, 3728.
- Arkhipov, V. I.; Bässler, H. *J Phys Chem* 1994, 98, 662.
- Monthus, C.; Bouchaud, J.-P. *J Phys A* 1996, 29, 3847.
- Vrentas, J. S.; Duda, J. L. *J Polym Sci: Polym Phys Ed* 1977, 15, 403, 417.
- Macedo, P. B.; Litovitz, T. A. *J Chem Phys* 1965, 42, 245.
- Kluin, J.-E.; Yu, Z.; Vleeshouwers, S.; McGervey, J. D.; Jamieson, A. M.; Simha, R.; Sommer, K. *Macromolecules* 1993, 26, 1853.
- Victor, J. G.; Torkelson, J. M. *Macromolecules* 1988, 21, 3490.
- Dalnoki-Veress, K.; Nickel, B. G.; Roth, C.; Dutcher, J. R. *Phys Rev E* 1999, 59, 2153.
- Ruan, M. Y.; Moaddel, H.; Jamieson, A. M.; Simha, R.; McGervey, J. D. *Macromolecules* 1992, 25, 2407.
- Yu, W.-C.; Sung, C. S. P.; Robertson, R. E. *Macromolecules* 1988, 21, 355.
- Yu, Z.; McGervey, J. D.; Jamieson, A. M.; Simha, R. *Macromolecules* 1995, 28, 6268.
- McKenna, G. B. in *Comprehensive Polymer Science*, Vol. 2; Booth, C.; Price, C., Eds., Pergamon Press: Oxford, 1989; p 311.
- Ferry, J. D. *Viscoelastic Properties of Polymers*, Wiley: New York, 1980.
- Turnbull, D.; Cohen, M. H. *J Chem Phys* 1961, 34, 120.
- Dean, G. D.; Tomlins, P. E.; Read, B. E. *Polym Eng Sci* 1995, 35, 1282.
- Bree, H. W.; Heijboer, J.; Struik, L. C. E.; Tak, A. G. M. *J Polym Sci: Polym Phys Ed* 1974, 12, 1857.

25. Struik, L. C. E. *Polymer* 1997, 38, 4053.
26. Plesset, M. S.; Zwick, S. A. *J Appl Phys* 1952, 23, 95.
27. Blumen, A.; Klafter, J.; Zumofen, G. *J Phys A* 1986, 19, L77.
28. Bouchaud, J. P. *J Phys I France* 1992, 2, 1705.
29. Bouchaud, J.-P.; Mezard, M. *J Phys A* 1997, 30, 7997.
30. Eyring, H. *J Chem Phys* 1936, 4, 283.
31. Drozdov, A. D. *Mechanics of Viscoelastic Solids*; Wiley: Chichester, 1998.
32. Tanaka, F.; Edwards, S. F. *Macromolecules* 1992, 25, 1516.
33. Green, A. E.; Naghdi, P. M. *Proc Roy Soc London* 1995, 448, 379.
34. Diezemann, G.; Mohanty, U.; Oppenheim, I. *Phys Rev E* 1999, 59, 2067.
35. Arkhipov, V. I.; Bäessler, H.; Khramtchenkov, V. D. *J Phys Chem* 1996, 100, 5118.
36. Kobayashi, Y.; Zheng, W.; Meyer, E. F.; McGervey, J. D.; Jamieson, A. M.; Simha, R. *Macromolecules* 1989, 22, 2302.
37. Ramachandra, P.; Ramani, R.; Ravichandran, T. S. G.; Ramgopal, G.; Gopal, S.; Ranganathaiah, C.; Murthy, N. S. *Polymer* 1996, 37, 3233.